



RESPONSE PREDICTION OF TYPICAL JAPANESE RC BUILDINGS CONSIDERING PARAMETRIC UNCERTAINTY

T. Yeow⁽¹⁾, K. Kusunoki⁽²⁾, H. Pan⁽³⁾

⁽¹⁾ Project Researcher, Earthquake Research Institute, University of Tokyo, trevoryeow@eri.u-tokyo.ac.jp

⁽²⁾ Professor, Earthquake Research Institute, University of Tokyo, kusunoki@eri.u-tokyo.ac.jp

⁽³⁾ Postdoc, State Key Laboratory of Internet of Things for Smart City, University of Macau, sherlock-4869@hotmail.com

Abstract

Response history analysis (RHA) is an integral part of modern structural engineering practice, particularly when having to consider complex dynamic loading such as earthquake or wind actions. However, engineers often do not have the time nor the resources to consider the influence of parametric uncertainty. This could result in unforeseen deformation modes (e.g. torsion), changes in strength hierarchy of the structural system (e.g. a soft-story mechanism forming instead of a more even spread of plasticity on different floors), and a significant increase in floor accelerations, among other effects. Furthermore, the Capacity Spectrum Method (CSM) is allowed as an alternative for buildings with heights less than 60 m in Japan and is also sensitive to parametric uncertainty. There is therefore a need to investigate the sensitivity of both approaches to the modelling parameters.

In this preliminary study, parametric sensitivity analyses were performed for a range of case study reinforced concrete buildings. These buildings are based on design examples provided by the Japan Building Disaster Prevention Association, which contains buildings of different span length, height and usage, and are typical of Japanese reinforced concrete frame buildings. Modelling parameters considered included concrete peak strength, steel reinforcing bar peak strength, mass eccentricity, and damping ratios. Structural analyses were performed on the CANNY software using Giberson elements for beams and multi-spring elements for columns. A set of five ground motions which have similar GMRot50 spectral shape to the Japanese design spectra were selected for analyses. Pushover analyses were also performed to obtain a “capacity curve” for use in CSM, while the 5% elastic acceleration-displacement spectra for the selected ground motions were adopted as the “demand curve”.

It was found that concrete peak strength and damping ratios had the greatest influence on the building’s drift and acceleration response, with a difference of up to almost 20% compared to the baseline structure in some cases. The former was due to concrete strength influencing several other parameters, such as concrete Young’s Modulus and tensile strength. In contrast, mass eccentricity did not have a significant effect as the load resisting frames were symmetric and reasonably well spaced out. Furthermore, increase steel strength had the smallest influence as it did not influence the building’s initial stiffness. In all cases considered, the deformation mechanism of the buildings was similar due to the consideration of overstrength actions in design following capacity design philosophy, indicating that the failure mechanism of a well-designed building should not be influenced by modelling parameters.

Results using CSM followed similar trends to those obtained from RHA. However, the peak interstory drifts considering all floors of the buildings from CSM were consistently larger. The percentage difference between the predicted values from CSM and RHA did not appear to be influenced by the modelling parameters adopted. However, building height had a significant influence on the percentage difference as CSM does not consider the influence of higher-order mode effects. Other aspects, such as spectral shape and energy dissipation were found to also heavily influence the difference in drifts predicted from RHA and CSM.

Keywords: Capacity Spectrum Method; Response History Analysis; reinforced concrete; uncertainty; parametric study



1. Introduction

Inelastic Response History Analysis (RHA) is an increasingly popular tool for modern structural engineering practice due to accessibility of RHA-capable software, particularly when having to consider complex dynamic loading such as earthquake or wind actions. However, engineers often do not have the time nor the resources to consider uncertainty in the selection of modelling parameters, such as material properties, damping ratios, and mass eccentricities. Instead, upper and lower bound values are often considered.

The Capacity Spectrum Method (CSM) [1] is allowed as an alternative to inelastic response history analysis in the Japanese Building Standard Law for buildings with heights less than 60 m [2]. This is done by performing a pushover analysis of the building, simplifying the response into a single-degree-of-freedom system, and finding the intercept between the capacity and demand curves accounting for P-delta and hysteretic damping effects. Similarly to RHA, the predicted response of the buildings using the Capacity Response Spectrum approach would also be sensitive to the modelling parameters.

Based on the above, there is a need to (i) determine the sensitivity of the building's response to various modelling parameter uncertainty, and (ii) assess the accuracy of CSM based on the modelling parameters. This preliminary study aims to address these needs by performing inelastic RHA and pushover analyses of a range of typical Japanese reinforced concrete (RC) buildings available from the Japan Architecture Disaster Prevention Association (JADPA) [3]. Four main parameters were considered; (i) concrete compression strength, (ii) damping ratio, (iii) mass eccentricity, and (iv) steel tensile strength. Other variables were not covered in this study.

2. Background

2.1 Material strength uncertainty

Shimizu et al. [4] tested 10,788 core samples obtained from 1,130 existing buildings in Japan. These buildings were constructed between 1926 and 1984, were used for educational or office purposes, and were between 1 to 10 floors high. However, over 90% of buildings sampled had a design concrete strength of 18 MPa or 21 MPa, which are much lower than the design strength values considered in JADPA [3]. Nonetheless, they showed that the compressive strength coefficient of variation, V_c , is generally smaller for newer buildings, with the average V_c being 0.25 in 1960 and 0.15 in 1980.

Bartlett and MacGregor [5] proposed that nominal concrete strengths, $F_{c,nominal}$, can be related to actual concrete strength, F_{cc} , following Eq. (1); where F_1 is the average ratio of cylinder strength to nominal strength and F_2 is the average ratio of in-situ strength to cylinder strength. V_c can be estimated following Eq. (2); where V_{F1} and V_{F2} are the coefficient of variation of F_1 and F_2 , respectively.

$$F_{cc} = F_1 \cdot F_2 \cdot F_{c,nominal} \quad (1)$$

$$V_c^2 = V_{F1}^2 + V_{F2}^2 \quad (2)$$

Wisniewski et al. [6] collated values of F_1 and F_2 from various literature from North America and Europe and had also derived values for F_1 based on data provided by the two largest precast concrete companies in Portugal. The proposed values using the new dataset are shown in Table 1, while they recommended using 0.85 and 10% for F_2 and V_{F2} , respectively.

Table 1 – F_1 parameter probabilistic distribution

Nominal strength (MPa)	F1	VF1
25	1.26	7.7%
30	1.18	7.5%
50	1.18	5.8%



For reinforcing steel strength, a large sample of steel bars had been tested by the General Building Research Corporation of Japan (GBRC) [7] to obtain probabilistic distribution of several steel reinforcing properties. The results of these for selected bar sizes are shown in Table 2.

Table 2 – Steel material property probabilistic distribution

Grade	Bar diameter (mm)	Sample size	Average tensile strength (MPa)	Standard deviation (MPa)
SD295A	10-22	243	358	16
SD345	16-32	857	390	13
SD390	25-38	7	433	8

2.2 Capacity Spectrum Method

The Capacity Spectrum Method [1] requires the derivation of a capacity curve and a demand curve, as the predicted building response is the intercept of the two curves. Kuramoto et al. [8] proposed a method to convert multi-degree-of-freedom (MDOF) pushover results to a representative single-degree-of-freedom (SDOF) curve using conventional modal analysis methods but considered the displacement shape at each step rather than the initial mode shapes. Kusunoki [9] proposed a method to further simplify the resultant SDOF curve into a trilinear curve so that the yield point can be used to assess the ductility demand.

To derive the demand curve, the elastic 5% damped spectral response curve is firstly required. The Japanese Building Standard Law Notification No. 1457-6 [10] prescribes a reduction factor, F_h , to then be applied to the elastic spectra to account for hysteretic damping effects as shown in Eq. (3). Here; h is the equivalent damping factor (calculated from Eq. (4) [11]), $h_{elastic}$ is the elastic damping factor, and μ is the response ductility. And illustration of this procedure is shown in Fig. 1.

$$F_h = \frac{1.5}{1 + 10h} \quad (3)$$

$$h = 0.25 \left(1 - \frac{1}{\sqrt{\mu}} \right) + h_{elastic} \quad (4)$$

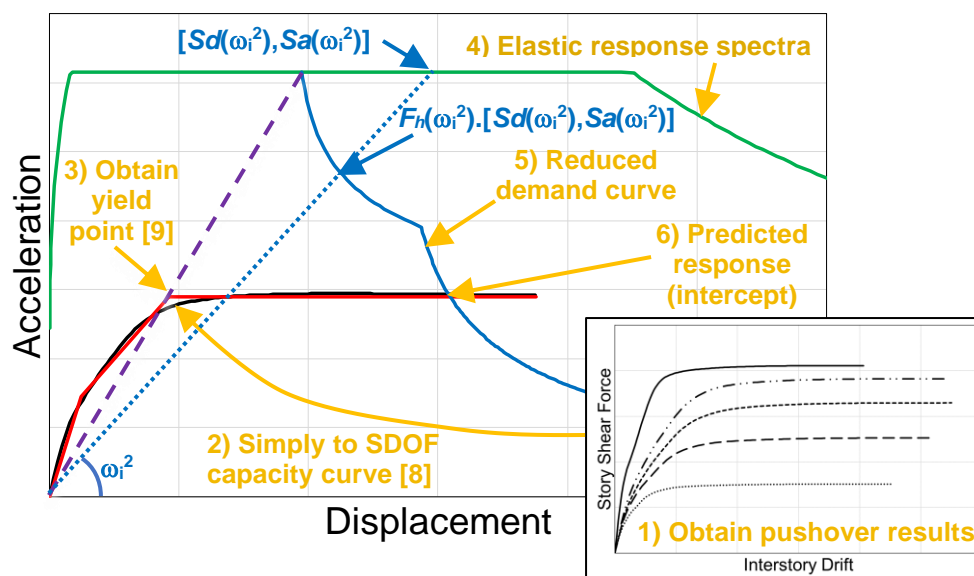


Fig. 1 – Illustration of the Capacity Spectrum Method approach



3. Case-study building information

Three case-study RC buildings were obtained from JADPA [3]. The buildings' generic layout are shown in Fig. 2, while the dimensions and number of floors are shown in Table 3. The cross-section dimensions are shown in Table 4, while the assumed nominal strength properties adopted in design are shown in Table 5.

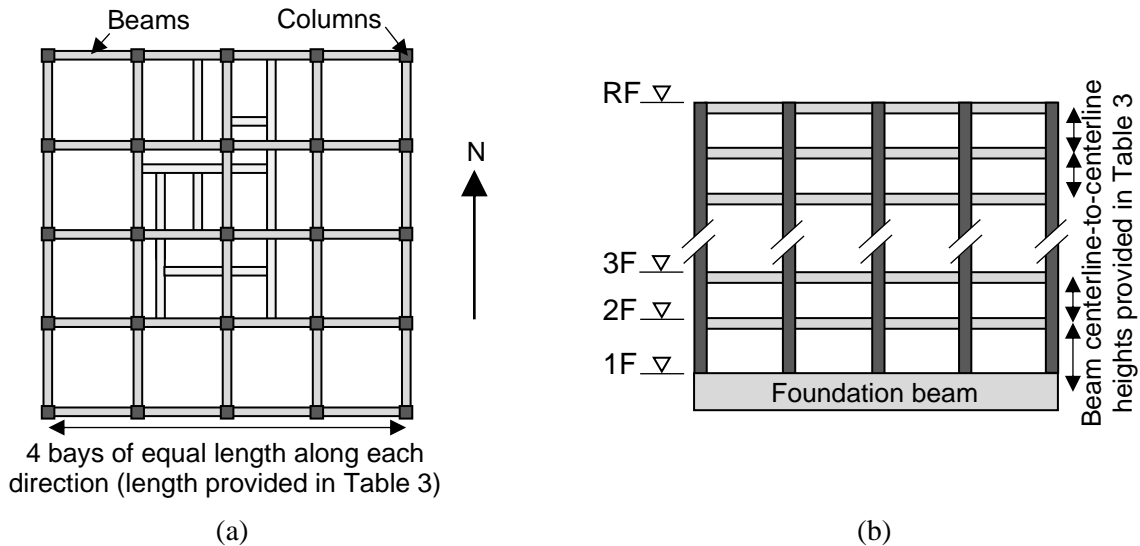


Fig. 2 – Case-study building; (a) plan elevation and (b) side elevation

Table 3 – Case study building dimensions (*average value)

Building ID	Number of floors	Span width (m)	Story height (m)		Weight (kN)		Book example reference
			1F-2F	Other	RF	Others	
A	5	6.0	3.41	2.86	8,420	10,200	1-9
B	14	6.0	4.11	3.02*	9,500*	10,600	1-11
C	5	7.6	3.46	2.94*	13,400*	15,200	1-13

Table 4 – Member dimensions (at specified floor level for beams, and above floor level for columns)

Element type	Section dimensions (mmxmm)	Building ID		
		A	B	C
Beams	500x700	ALL	-	5F-RF
	550x800	-	13F-RF	2F-4F
	600x850	-	7F-12F	-
	650x900	-	2F-6F	-
Column	850x850	ALL	13F-14F	ALL
	900x900	-	10F-12F	-
	950x950	-	4F-9F	-
	1000x1000	-	1F-3F	-



Table 5 – Nominal material strengths adopted in design

Material	Nominal strength	Notes
Concrete	24 MPa	Whole building (A and C), 13 th floor or higher (B)
	27 MPa	11 th to 13 th floor (B only)
	33 MPa	7 th to 11 th floor (B only)
	36 MPa	Foundation to 7 th floor (B only)
Steel	295 MPa	10-16 mm bars
	345 MPa	19-29 mm bars
	390 MPa	32 mm or larger bars

4. Methodology

4.1 Structural analysis and member modelling

The structural analyses were performed on the CANNY software [12] using Rayleigh tangent stiffness damping model on 1st and 3rd modes and large displacement analyses. The program uses Gibson elements for beams, while multi-spring elements were selected for columns. CS4 and SS3 hysteretic models from the CANNY software [12] were adopted for concrete and steel materials, respectively. The backbone of the two materials are shown in Fig. 3. Here, F_{cc} , F_{ct} , and F_s are the peak strengths corresponding to concrete compression, concrete tension, and steel strength (same in compression and tension), respectively; E_c and E_s are the Young's Modulus for concrete and steel, respectively; ε_{cc} and ε_{cu} are the strains at peak concrete compression and at concrete failure, respectively; ε_{sy} and ε_{su} are strains at yield and failure of steel, respectively; and λF_{cc} is the residual concrete strength capacity. For simplicity, $\varepsilon_{cu}/\varepsilon_{cc}$ was taken as 5.0 while λ was taken as 0.2. Furthermore, E_s was taken as 200 GPa and β was assumed to be 0.001.

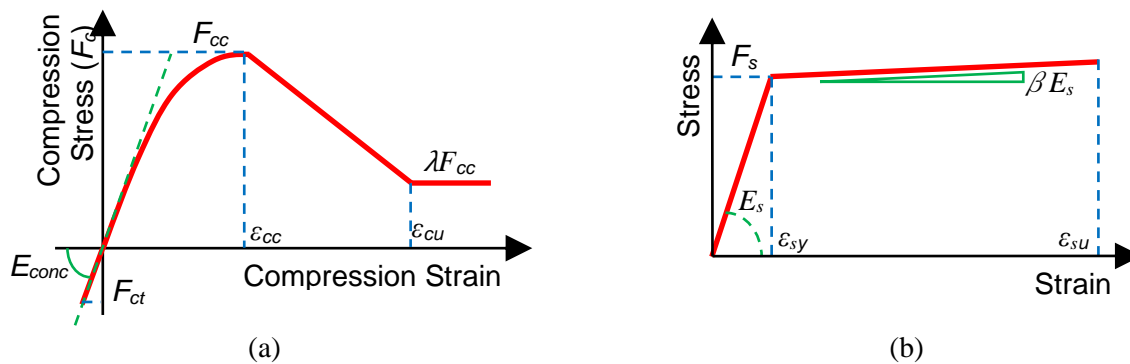


Fig. 3 – Backbone shapes of adopted material models; (a) concrete, and (b) steel

The equation used to model the concrete compression stress-strain relation from the origin to ε_{cc} is shown in Eq. (5). The equations to estimate ε_{cc} , E_c , and F_{ct} and were adopted from Chang and Mander [13], Noguchi and Tomosawa [14], and ACI 318 [15], respectively, and are shown in Eqs. (6)-(8). Note that the concrete mass density was assumed to be 2.3 t/m³.

$$F_c(\varepsilon) = E_c \varepsilon_{cc} \left[\frac{\varepsilon}{\varepsilon_{cc}} - \left(\frac{E_c \varepsilon_{cc} - F_{cc}}{E_c \varepsilon_{cc}} \right) \left(\frac{\varepsilon}{\varepsilon_{cc}} \right)^{\frac{E_c \varepsilon_{cc}}{E_c \varepsilon_{cc} - F_{cc}}} \right] \quad (5)$$

$$\varepsilon_{cc} = \frac{F_{cc}^{0.25}}{1150} \quad (6)$$



$$E_c = 3.35 \times 10^4 \cdot \left(\frac{\gamma}{24}\right)^2 \cdot \left(\frac{F_{cc}}{60}\right)^{1/3} \quad (7)$$

$$F_{ct} = 0.56\sqrt{F_{cc}} \quad (8)$$

4.2 Ground motion selection

Ground motion records were selected from the PEER Ground Motion Database (over 3,000 set of records as of December 2016) [16] based on the median response spectra considering all possible rotation angles of orthogonal horizontal recordings, GMRot50 [17] to match the Japanese Building Code spectra between periods of 0.01 s and 3.0 s. For each record; (i) GMRot50 spectra was derived, (ii) the scale factor was varied from 0.5 to 2.0 in steps of 0.1, (iii) the error between the scaled GMRot50 spectra and the target spectrum was computed using square-root-of-sum-squares of the logarithmic values, and (iv) the scale factor corresponding to the smallest error was selected for the given record. Once this was done for all records, the database was sorted according to the error. Five records from distinct events with the lowest error were then selected for RHA and deriving the demand curve for CSM. These are shown in Table 6 while the spectrums are shown in Fig. 4.

Table 6 – Selected ground motion records

NGA ID	Event	Recording station/location	Scale factor
182	Imperial Valley 1979	USGS Station 5028	1.59
776	Loma Prieta	CDMG Station 47524	2.00
821	Erzikan 1992	-	1.34
1085	Northridge 1994	Sylmar Converter Station East	1.20
1504	Chi-Chi 1999	TCU067	1.44

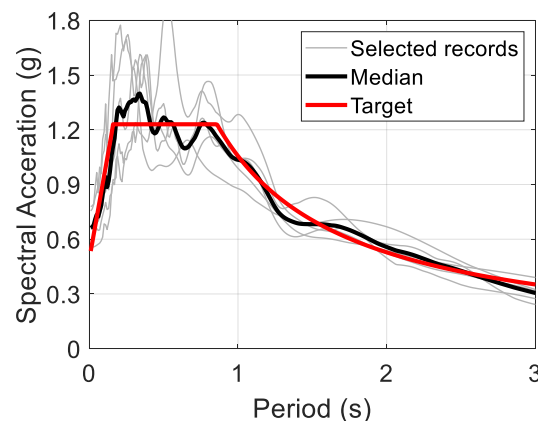


Fig. 4 – Comparison of acceleration spectra of selected records with target spectra

4.3 Parametric uncertainty

Five cases will be considered in this study as follows:

- I) Baseline building
- II) Increased concrete strength
- III) Decreased damping ratio
- IV) Increased mass eccentricity



V) Increased steel strength

For concrete compression strength, the nominal value is often considered in numerical modelling in practice. These were generally lower than the 16th percentile values obtained from Wisniewski et al. [6] (assuming $F_2 = 1.0$) as shown in Table 7 and was thus adopted for the “baseline” building (Case I). The 84th percentile values will be adopted for the building with “increased concrete strength” (Case II).

Table 7 – Concrete compression strength 16th and 84th percentile values [6]

Nominal strength	F1	VF1	VF2	Mean strength	Standard deviation	16 th percentile	84 th percentile
24 MPa	1.28	7.74%	10%	30.6 MPa	3.9 MPa	26.7 MPa	34.5 MPa
27 MPa	1.23	7.62%	10%	33.2 MPa	4.2 MPa	29.0 MPa	37.3 MPa
33 MPa	1.18	6.99%	10%	38.9 MPa	4.8 MPa	34.1 MPa	44.7 MPa
36 MPa	1.18	6.48%	10%	42.5 MPa	5.1 MPa	37.4 MPa	47.5 MPa

Damping ratios and mass eccentricities often adopted in numerical modelling are 5% and 0% for regular symmetric buildings, respectively. These two values were adopted for the “baseline” building. Depending on various factors, the damping ratio could be as low as 3% or much greater than 5%. For conservatism, 3% damping was adopted for the building with “decreased damping ratio” (Case III). With regards to mass eccentricity, many codes often recommend considering 10% (i.e. mass is offset by 10% of the building’s width), and thus this was considered for the building with “increased mass eccentricity” (Case IV).

Finally, 1.1 times the nominal steel strength is often assumed as a lower bound value. This was lower than the 16th percentile value from Table 8 (based on GBRC [7]) for Grade SD295A, but greater for SD345 and SD390. For simplicity, the 16th percentile values for all steel grades were adopted for the “baseline” building. The 84th percentile values were adopted for the building with “increase steel strength” (Case V).

Table 8 – Steel properties 16th and 84th percentile values [7]

Grade	Yield strength (MPa)				Elongation at fracture (%)			
	Mean	Standard deviation	16 th percentile	84 th percentile	Mean	Standard deviation	16 th percentile	84 th percentile
SD295A	363	15	348	378	27	2.1	24.9	29.1
SD345	388	13	375	401	27	2.6	24.4	29.6
SD390	432	8	424	440	23	2.0	21.0	25.0

5. Structural Analysis Results

5.1 Single-degree-of-freedom pushover curves

The SDOF pushover approximation in the EW direction derived from pushover analysis following Kuramoto et al. [8] is shown in Fig. 5. The stiffest building of all cases was from increasing the concrete strength. This is due to several parameters being influenced by concrete strength as shown in Eqs. (6)-(8). The strongest building was from increasing the steel strength. Changing the mass eccentricity had little influence on the SDOF pushover, though it did result in some out-of-plane response which is not reflected in the SDOF curves. Decreasing damping ratio had no influence since it had no effect on the building’s strength and stiffness.

Building A was the strongest (in-terms of representative acceleration) and stiffest of all three buildings. Both Building B and Building C have similar strengths, but Building B was much more flexible with a yield displacement of approximately 0.15 m compared to Building C with approximately 0.05 m. Therefore, the



spectral acceleration demand would be lower for Building B compared to Building C, resulting in lesser inelastic response.

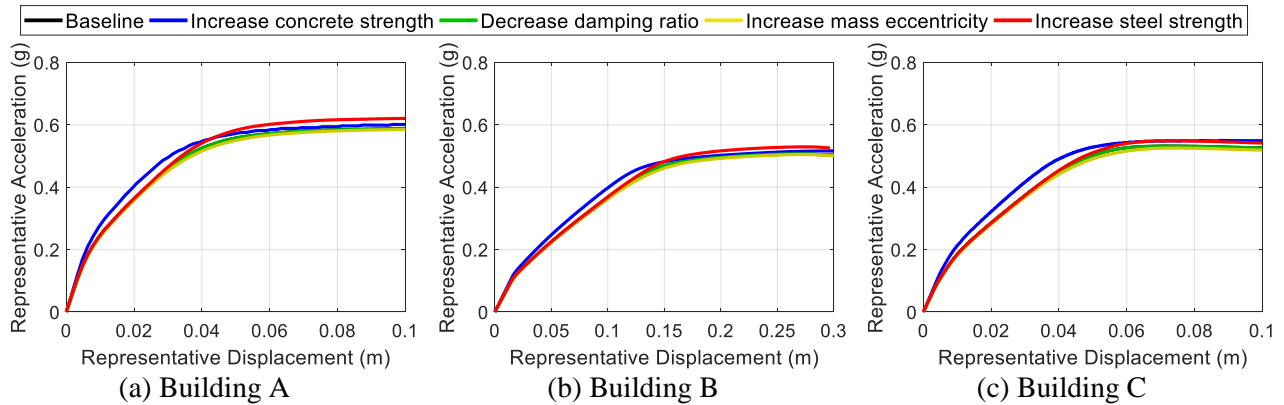


Fig. 5 – Trilinear approximation of pushover curves (EW direction)

5.2 Median drift profiles

The median drift profiles measured at the centroid of each floor considering all 5 records and both horizontal components are shown in Fig. 6. In all cases, the drift response is similar regardless of mass eccentricity or if the steel strength was increased. While torsion increased the building's response in some cases, there were others where torsional effects caused by excitation in one horizontal direction acted against torsional effects caused by the orthogonal direction; resulting in the median response not increasing significantly. Increasing steel strength did not have any influence on other parameters such as building stiffness. If one assumes the Equal Displacement rule, the resulting displacement response would be similar if the initial period is consistent. In contrast, increasing concrete strength caused the drift response to decrease due to several parameters being influenced by this parameter as discussed from Fig. 5. Finally, decreasing the damping ratio resulted in the building's drift response increasing as expected.

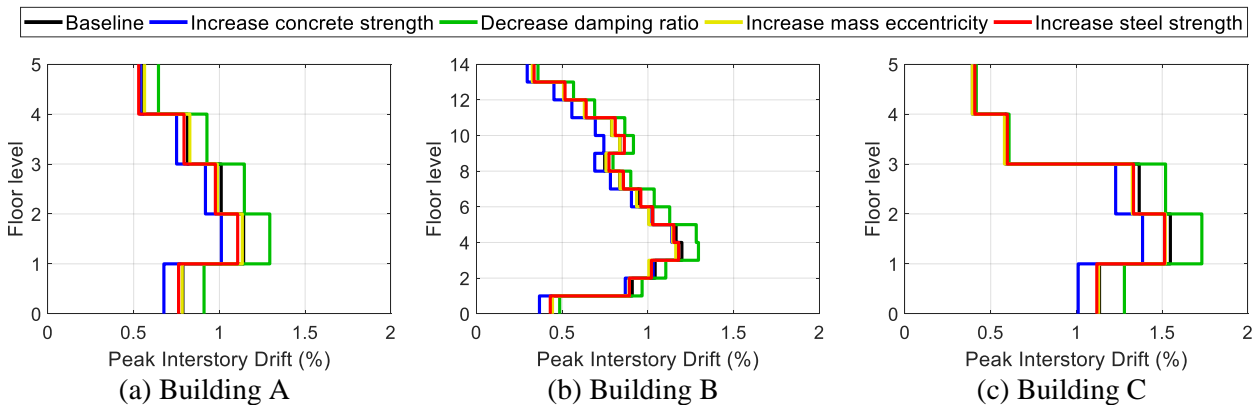


Fig. 6 – Estimated median building interstory drift from Response History Analysis

5.3 Sensitivity of response to selected parameters

The absolute percentage difference between the maximum recorded peak interstory drift considering all floors in the building from each case to the baseline building is shown in Fig. 7. It should be noted that the average (avg) value shown is the average percentage difference observed from each record, and not the percentage difference of the median drift profiles from Fig. 6. In most cases, decreasing the damping ratio had the greatest influence overall. Increasing concrete strength had the second greatest effect due to this parameter influencing several other structural properties as discussed previously. The effect of increasing mass eccentricity appeared to be more significant for taller (Building B) or weaker/flexible (Building C) buildings. Increasing steel strength generally had the lowest effect. Interestingly, the effect of mass eccentricity appeared to have a greater



influence on the percentage difference in Fig. 7. than the median drift profile observed in Fig. 6. This was likely due to torsion increasing the response in some cases and decreasing it in others, resulting in a similar median despite having noticeable differences.

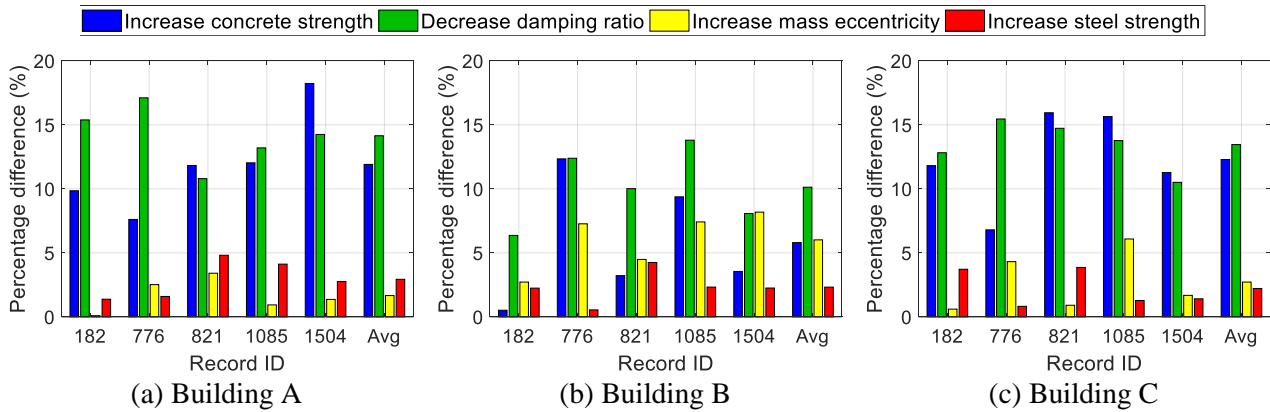


Fig. 7 – Percentage difference in building peak interstory drift

6. Capacity Spectrum Method Predictions

6.1 Comparison of predicted drift response

The pushover curves from Fig. 5 were further simplified into a trilinear curve following Kusunoki [9] and were used to predict the representative displacement for each building and record considered following CSM outlined in Section 2.2. The representative displacements were then converted back to drifts. The median of these drifts for each building are shown in Fig. 8. In general, the drifts for Buildings A and C were greater than those predicted from inelastic response history analyses (Fig. 6), indicating a more conservative estimate. Building B had larger drifts on the lower half of the building, but smaller drifts on upper floors. However, the effect of changing parameters was similar, where increasing concrete strength resulted in the smallest response, decreasing damping ratio resulted in the largest response, and the response for the other three cases are similar.

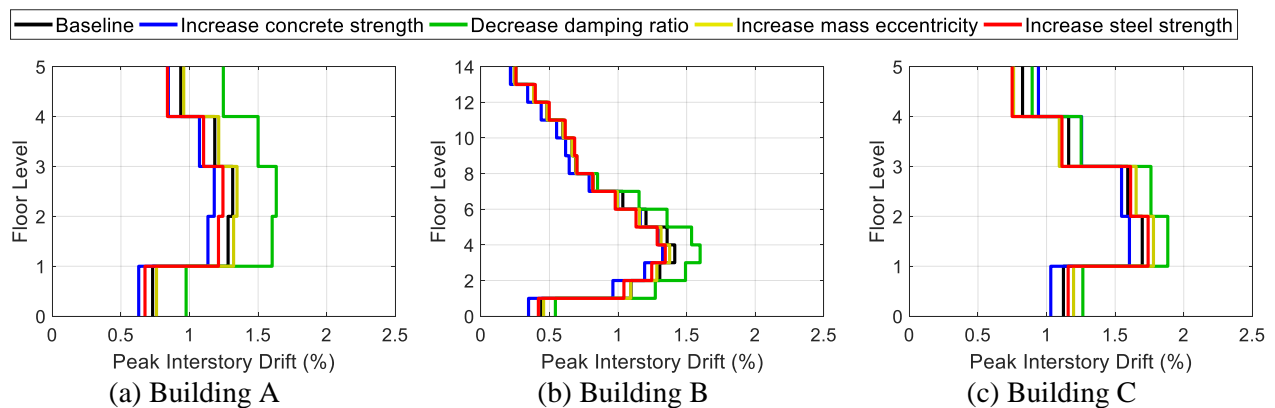


Fig. 8 – Estimated median drifts using the Capacity Spectrum Method approach

6.2 Sensitivity of accuracy to selected parameters

The difference in the largest predicted drift for each building and record (considering both horizontal components) between CSM and RHA are shown in Fig. 9. The error was generally around 20% or less for Buildings A and C, except for several cases using NGA821 and NGA1504 records. Overall, there was no consistent trend where modifying a single parameter resulted in varying differences between the two methods. In contrast, there are much greater differences for Building B where the average difference was 30% or greater.

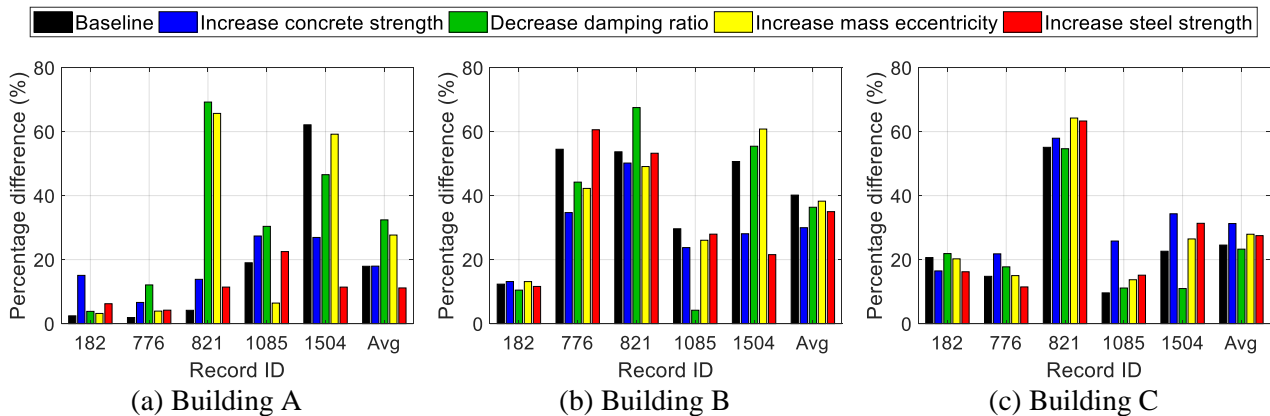


Fig. 9 – Prediction difference between Capacity Spectrum Method and Response History Analysis

7. Discussion

7.1 Parametric uncertainty for RHA

One limitation in this study was that the upper and lower bound values were applied to the entire building at the same time. It is possible that a mix of values, such as a higher percentile strength in beams and a lower percentile strength in columns, could result in a different mode of failure such as soft-story or shear. However, it can be argued that if the building was adequately designed following capacity-design procedures, the probability of this occurring is small.

Other structural parameters which were not examined here, such as post-elastic stiffness and choice of damping model, could also influence the building's response. The influence of ground motion parameters, such as energy content and duration, are also important. The influence of these parameters as well as the potential for different failure modes to occur will be examined in future extensions of this study.

7.2 Reasons for difference in predicted drifts between CSM and RHA

Based on the findings in this study, the CSM generally predicted higher drifts compared to RHA for the range of buildings and ground motions considered. One reason of this could be due to using the secant stiffness corresponding to the yield point when determining the influence of hysteretic damping. In reality, there could be some further energy dissipation prior to reaching the yield point. Consideration of this effect would result in the spectral demands being reduced earlier, thus potentially reducing the demand. This effect could be more pronounced if the building's response was highly influence by the first few cycles of shaking.

Another reason could be due to the shape of the spectral demand. Consider the response prediction for Building A's "baseline" case (Case I) and "increasing steel strength" case (Case V) for NGA1504 NS direction shown in Fig. 10. The baseline case came close to intercepting the demand curve at approximately 0.118 m, but the actual interception point was at 0.135 m. In contrast, the intercept did occur at approximately 0.118 m when increasing steel strength. This accounted for the large difference observed in Fig. 9a for this case. This effect had been noted in past studies [18].

The final potential reason was due to higher-mode effects, which would influence taller buildings more than shorter buildings, resulting in the larger error observed for Building B. In this case, higher-order mode effects could cause larger drifts to occur on upper floors, which help dissipate energy and thus reduce drifts on lower floors. For the baseline case, Building B required the consideration of the first three modes to reach a cumulative effective mass ratio of 90%, whereas only the first two were required for Buildings A and C. Furthermore, the ratio of spectral displacements between the elastic initial first and second mode was approximately 8.8 for Building B, compared to 19.7 and 12.2 for Buildings A and C, respectively. This implied that not only are more modes contributing to Building B's response, but the size of the contribution was also larger, resulting in the greater difference observed for this case.



- [6] Wisniewski DF, Crus PJS, Henriques AAR, Simoes RAD (2012): Probabilistic models for mechanical properties of concrete, reinforcing steel and pre-stressing steel. *Structure and infrastructure engineering*, **8**(2), 111-123.
- [7] General Building Research Corporation of Japan (2005): Test result statistics for construction materials in the fiscal year of 2004: part 2 Deformed reinforcing bars and their connections. GBRC, Osaka, Japan.
- [8] Kuramoto H, Teshigawara M, Koshika N, Isoda H (2001): Conversion of multi-story building into equivalent SDOF system and its predictability for earthquake response (in Japanese), *Journal of Structural and Construction Engineering*, **66**(546), 79-85.
- [9] Kusunoki K (2019): Analytical study on the extrapolation method for the performance curves of R/C structures derived from recorded accelerations. *Journal of Structural and Construction Engineering*, **84**(761), 961-971.
- [10] Ministry of Land, Infrastructure, Transport and Tourism (2000): Notification No. 1457-6. *Technical Standard for Structural Calculation of Response and Limit Strength of Buildings*, Tokyo, Japan.
- [11] Shibata A, Sozen MA (1976): Substitute structure method for seismic design in RC. *Journal of the Structural Division*, **102**, 1-18.
- [12] Li K (2016): CANNY for three dimensional nonlinear static and dynamic structural analyses (version C2016.086)
- [13] Chang GA, Mander JB (1994): Seismic energy-based fatigue damage analysis of bridge columns: part 1 – evaluation of seismic capacity. *NCEER Technical Report No. NCEER-94-0006*, State University of New York, Buffalo, N.Y., USA.
- [14] Noguchi T, Tomosawa F (1995): Relationship between compressive strength and modulus of elasticity of high strength concrete (in Japanese). *Journal of structural and construction engineering*, **474**, 1-10.
- [15] American Concrete Institute (2014): ACI committee 318 – building code requirements for structural concrete and commentary. American Concrete Institute, MI, USA.
- [16] Chiou BSJ, Darragh R, Gregor N, Silva W (2008): NGA Project Strong-Motion Database. *Earthquake Spectra*, **24**(1), 23-44.
- [17] Boore DM, Weston-Lamprey J, Abrahamson NA (2006): Orientation-independent measures of ground motion. *Bulletin of the seismological society of America*, **96**(4a), 1502-1511.
- [18] Faella G, Giordano A, Mezzi M (2004): Definition of suitable bilinear pushover curves in nonlinear static analyses. *13th World Conference on Earthquake Engineering*, Vancouver, Canada.